FACTA UNIVERSITATIS (NIŠ)
Series: Electronics and Energetics vol. 1(1995), 11–27

DESIGN OF THE OBSERVER-BASED SPEED CONTROLLER APPLIED IN SERVO DRIVESWITH LIMITED RESOLUTION OF POSITION SENSORS

Milić Stojić and Slobodan Vukosavić

Abstract. This paper deals with the design of observer-based controller for high-performance speed-controlled servo drives that employ incremental encoders for sensing of the motor shaft position. The suggested extended observer is designed by introducing the additional integration state variable within the ordinary identity observer in order to enable, even in the presence of a constant or slow varying load torque disturbance, the estimation of shaft speed and filtering of position signal contaminated by the quantization noise due to a limited resolution of position transducer. The useful procedures for setting of controller parameters and adjustment of observer gains are proposed.

1. Introduction

High performance servomechanisms employ position sensors on the motor shaft [1,2]. In practice, two types of sensors are most frequently applied: optical encoders (absolute or incremental), and electromagnetic resolver. In the case of an absolute optical encoder, the shaft position is read as a digital word obtained directly from the sensor. On the other hand, the incremental encoder must be equipped with an up-down counter driven by the encoder pulses "A" and "B". This counter can be set to the position "0" each time when the marker "C" of the incremental encoder appears. Finally, the shaft position is read as an digital word, as well. The electromagnetic resolver generates sinusoidal voltages at the detection windings; amplitudes and phases of these voltages are related with the shaft position. At the output register or the resolver–to–digital (R/D) converter, which comprises the closed–loop

Manuscript received December 23, 1993.

The authors are with the Electrical Engineering Faculty, University of Belgrade, Bulevar Revolucije 73, 11000 Belgrade.

PLL-based position tracking, the shaft position is also read in the form of a digital word. Hence, the resolution of the shaft position measurement is limited in all cases. The limit depends upon the specific application and sensor technology.

In robotics applications, a number of motors is attached to moving parts. Requirements for the fast operation and as short as possible cycle times impose the claim for light robot arms. Moreover, the restricted room and limited weight of the motor call for the operation at raised temperatures. Therefore, the usage of optical shaft sensors is not advisable and thus, in servos for robot hands, robust electromagnetic resolvers are commonly used for sensing the shaft position. Up to date resolvers and R/D converters enable the detection of shaft position with (12-14)-bit resolution for high–speed motors, and 16-bit resolution in the case of low-speed (direct drive) motors. The resolver generates the position feedback signal, which is also used as an input signal for the torque control of AC motors: in indirect field orientation schemes for induction motors, and current vector orientation for brushless DC motors. The signal from position transducer is often used to estimate the velocity signal necessary for the design of high-performance servos [1,2].

As it has been shown [1,2], for the torque control of AC motors [3] (field/current vector spatial orientation), the 8-bit resolution of the shaft position signal is quite sufficient. On the other hand, the resolution of position signal used for the speed- and position-feedback purposes is crucial for the overall performance of a servomechanism. Due to the finite resolution, the actual shaft position differs from the digital word representing the position (the lower resolution, the larger difference). Therefore, both the position error and the speed estimate are contamined by a quantization noise. In the compensation of error signal, controller gains amplify pulsations and thus generate a fluctuating torque command. As the result, the shaft position will not be smooth as necessary, speed and position of the shaft will oscillate, and motor losses will increase due to the pulsating current. Sometimes, in practice, controller gains are reduced in such instances, and the error signal (or the torque reference) is filtered. This resolves the problem of torque pulsations produced by the finite resolution of the position sensor; but, both of the aforementioned actions reduce the bandwidth of the closed–loop speed- or position–control system. Consequently, the speed of system response reduces and thus the cycle time of the relevant operation of the robot arm often becomes unacceptable. At the same time, due to reduced gains, the drive "stiffness" is lower; hence, the drive becomes substantially

sensitive to load torque disturbances.

To increase the bandwidth of closed–loop servo system or the speed of system response and to remove as much as possible undesirable effects of load torque disturbances, the controller sampling time has to be reduced, and controller gains must be increased. To this end, the key factor that is getting worse the drive performance becomes the "object (drive)-digital controller" interface or, in particular, the resolution of the shaft-position measurement and the quality shaft-velocity estimation.

In order to obtain smooth and sufficiently accurate position and speed signals, an observer structure is often implemented. Recall, the observer processes the torque command and a quantized signal from the position transducer. The observer structure including assumed parameters of the mechanical subsystem (such as the inertia and friction) is design to simulate the mechanical portion of the drive. In the observer, the shaft and position signals are estimated with a extended resolution; essentially, the resolution of these signals is limited only by the wordlenght of variables within the digital controller/signal processor. Observer gains multiply the error between the output of position transducer and the position estimate calculated by the observer, and the observer is designed to eliminate uncertainties that might appear in velocity and position estimates due to mismatched parameters and the influence of an unknown load torque.

This paper deals with the analysis and design of the observer-based speed and position controllers, in an environment where the shaft position information is incomplete due to a limited resolution of the position transducer [4]. In robotics applications, the employed observer must enable the estimation of the plant state variables even in the case of the constant (gravitation) or a slow varying load torque disturbances. Namely, in the regime of high load torque or high operating speeds, the position signal and other estimated variables derived by the observer must not differ from their actual values in the steady state. We discuss the possibility of employing the discrete–time velocity observer with additional state integrator [4]. The solution consists in the following: the observation error vector is multiplied be the observer gain matrix, while the error of position estimation is simultaneously processed through the discrete integrator assuring the zero steady-state estimation error, in the presence of a constant load torque disturbance.

In this paper, the setting of observer gains and adjustment of servo controller parameters are accomplished simultaneously. Even though the observer is decoupled from the drive dynamic, the performance of the speed/po-

sition controller is strongly affected by the observer design. In that regard, the observer may be viewed as an low-pass filter within the main control loop of the servo system, and therefore both the observer gains and controller parameters must be fitted in accordance with the desired dynamic performance of the overall system comprising the servo drive and observer. Guidances are given for selecting of controller parameters in accordance with the desired stability margin and the achievable speed of closed-loop system response, and the method of adjustment of observer gains is developed to optimally reduce torque ripples caused by the quantization noise present in the measured position input command and to achieve the desired speed of convergence to the same position values as measured.

2. Setting of Controller Parameters

Fig. 1. shows a simple structure of the speed–controlled drive with the electrical motor having the inertia J.

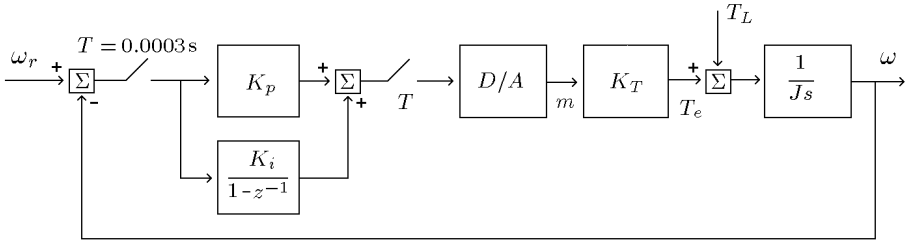

Fig. 1. Structure of speed-controled electrical drive

High–performance electrical drives (with the vector–controlled induction motors or brushless motors, for example) are usually equipped with electromagnetic torque controllers that reveal a relatively small torque response times that may be neglected when compared with the time constant of mechanical portion of speed- or position–controlled servosystems [1]. Hence, in a linear regime of operation, the generated electrical torque may be considered proportional to the torque command, $K_e(t) = K_T m(t)$, where K_T denotes the torque constant. For the regulation of the motor shaft speed, the conventional digital PI controller with the proportional and integral gains (K_P and K_I) is applied. In the plant of the system in Fig. 1., $\omega_r, \omega, T_L(t)$, and T denote respectively the speed reference, shaft speed, load torque disturbance, and sampling period.

For the sake of clarity in further developments, we will first determine the values of controller parameters K_P and K_I that match the desired continuous–time step response of the system. Note, due to the separation principle [5,6], values of controller parameters and appropriate gains of the associated observer can be determined separately.

For $T_L \equiv 0$, the z-transform of the motor speed is obtained from Fig. 1 as

$$\begin{aligned}\Omega(z) =& \mathcal{Z}\Big[\frac{1-e^{-Ts}}{s}K_T\frac{1}{Js}\Big]M(z)\\ =&(1-z^{-1})\mathcal{Z}\Big[K_T\frac{1}{Js^2}\Big]M(z)\\ =&C\frac{1}{z-1}\end{aligned} \tag{1}$$

where $C = K_T T/J$ denotes the parameter characterizing the plant of system under consideration. The parameter can be measured on a real system by a simple experiment.

With (1), the characteristic equation of the system in Fig. 1. becomes

$$1 + K_P C\frac{1}{z-1} + K_I C\frac{z}{(z-1)^2} = 0$$

or

$$z^2 + (K_P C + K_I C - 2)z + 1 - K_P C = 0. \tag{2}$$

The values of controller parameters can be easily obtained according to the desired stability margin and speed of continuous–time system response determined respectively by the relative damping coefficient ξ and natural frequency ω_n of the system dominant pair of poles inside the principal strip of the s-plane [7]. Thus, by equating identically the coefficients of equation

$$z^2 - 2\exp(-\xi\omega_n T)\cos(\xi\omega_n T\sqrt{1-\xi^2})z + \exp(-2\xi\omega_n T) = 0 \tag{3}$$

with the corresponding coefficients in (2), one obtaines

$$\begin{aligned}K_P C + K_I C - 2 &= -2\exp(-\xi\omega_n T)\cos(\xi\omega_n T\sqrt{1-\xi^2}),\\ 1 - K_P C &= \exp(-2\xi\omega_n T),\end{aligned} \tag{4}$$

wherefrom we get

$$K_P = \frac{1}{C}\Big[1 - \exp(-2\xi\omega_n T)\Big], \tag{5}$$

$$K_I = \frac{1}{C}\Big[1 - 2\exp(-\xi\omega_n T)\cos(\xi\omega_n T\sqrt{1-\xi^2}) + \exp(-2\xi\omega_n T)\Big]. \qquad (6)$$

The speed–controlled servo for the robot hand with $T = 0.0003s$ and $C = 0.15$ is considered. Assigning $\xi = 0.6$ and the bandwidth of closed–loop system $f_c = 50Hz$ ($\omega_n \cong 2\pi f_c$), from (5) and (6), we calculate $(K_P, K_I) = (0.7129, 0.056)$. For example, if the aperiodical step response with $\xi = 1$ and $\omega_n = 2\pi f_c = 314.159rad/s$ is desired, then relationships (5) and (6) yields $(K_P, K_I) = (1.1453, 0.0539)$.

The system in Fig. 1. was simulated in details taking into account quantization effects within the digital controller. The result of simulation run for $(K_P, K_I) = (0.7129, 0.056)$ is shown in Fig. 2. From the figure, one can easily conclude that the speed of continuous–time system step response and system stability margin match the assigned ones.

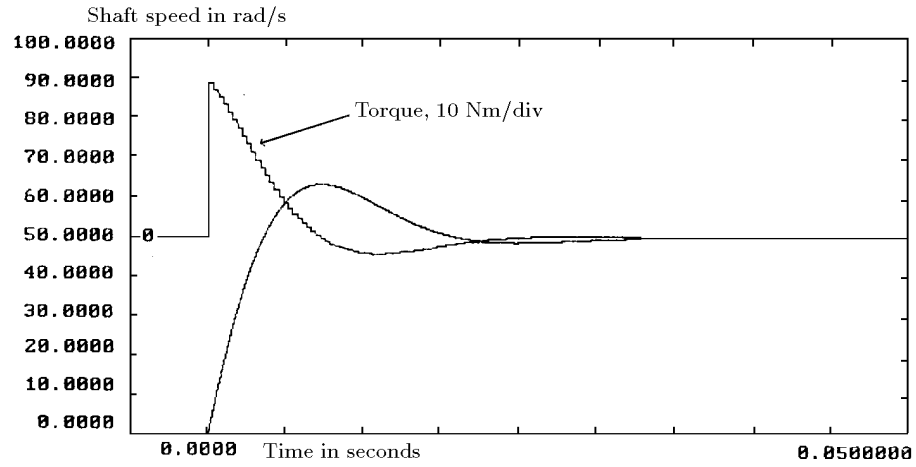

Fig. 2. Step response and torque command of speed-controled drive

3. Design of Identity Observer

The structure of observer–based speed–controlled drive is shown in Fig.3. The continuous portion of controlled system comprises the digital–to–analog converter (D/A), electromagnetic torque controller with torque constant K_T, motor, and position transducer (electromagnetic resolver with resolver–to–digital converter).

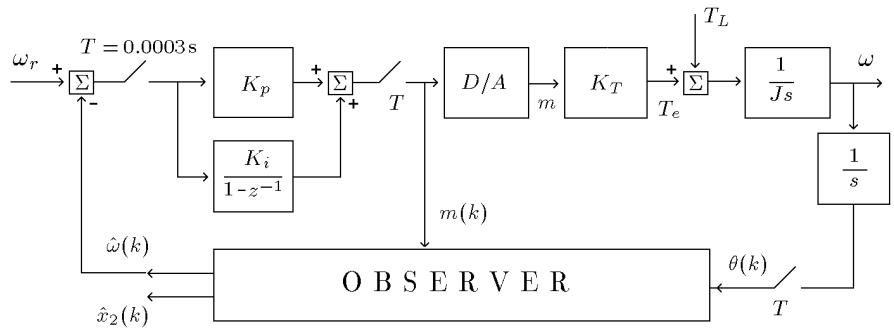

Fig. 3. Structure of observer–based speed-controled drive

For $T_L(t) \equiv 0$, the z-transform of the shaft angle is calculated from Fig. 3. as

$$\begin{aligned}\Omega(z) =& \mathcal{Z}\Big[\frac{1-e^{-Ts}}{s} K_T \frac{1}{Js^2}\Big] M(z) \\ =& (1-z^{-1})\mathcal{Z}\Big[K_T \frac{1}{Js^3}\Big] M(z) \\ =& \frac{K_T T^2}{2J} \frac{z^{-1}(1+z^{-1})}{(1-z^{-1})^2} M(z).\end{aligned} \tag{7}$$

In virtue of (7), the discrete model of the plant may be represented by the block notation and simulation diagram in Fig. 4. (a) and (b), respectively.

By assuming state variables as outputs of delay elements in Fig. 4. (b), the state and output discrete equations of the plant become

$$x(k+1) = E(T)x(k) + f(T)m(k), \tag{8}$$

$$\theta(k) = D(T)x(k) \tag{9}$$

with

$$E(T) = \begin{bmatrix} 1 & 0 \\ T/2 & 1 \end{bmatrix}, \tag{10a}$$

$$f(T) = \begin{bmatrix} K_T T/J \\ 0 \end{bmatrix} \tag{10b}$$

and

$$D(T) = \begin{bmatrix} T/2 & 2 \end{bmatrix}. \tag{10c}$$

Notice, the first and second state variables represent respectively the shaft speed $[x_1(k) = \omega(k)]$ and a linear combination of $\omega(k)$ and the shaft position $\theta(k)$ $[x_2(k) = \frac{1}{2}\theta(k) - \frac{T}{4}\omega(k)]$.

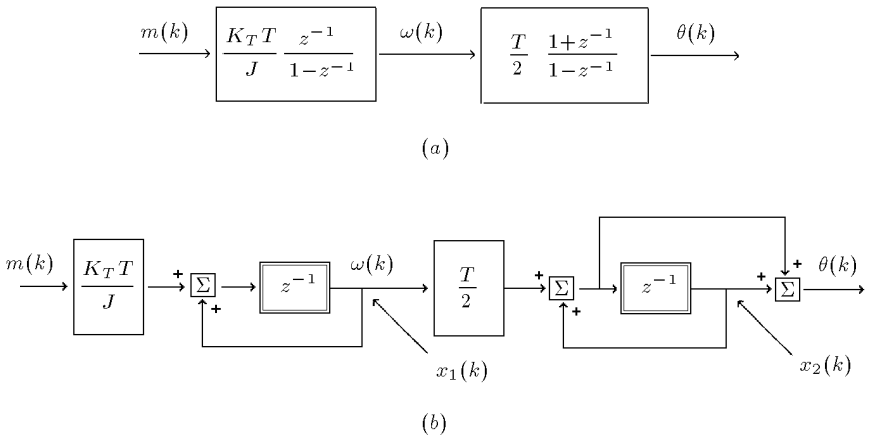

Fig. 4. a) Discrete model of the plant b) Simulation diagram

The observer design is accomplished directly from the observer equation [5,6]

$$\hat{x}(k+1) = (E - KD)\hat{x}(k) + K\theta(k) + fm(k) \tag{11}$$

where $\hat{x}(k) = [\,\hat{\omega}(k) \quad x_2(k)\,]^T$ and $\theta(k)$ are the vector of observed variables and measured angle position, respectively; K is the observer gain matrix

$$K = [\,K_1 \quad K_2\,]^T \tag{12}$$

which is to be determined according to requirements for the desired speed of estimation of state variables and minimization of system sensitivity with respect to a quantization noise within the digitai controller and observer.

After substituting $E = E(T),\ f = f(T),\ D = D(T)$, and K from (10) and (12) into (11), the observer equation (11) may be rewritten in the form

$$\begin{aligned} \hat{\omega}(k+1) &= (1 - K_1\frac{T}{2})\hat{\omega}(k) - 2K_1\hat{x}_2(k) + K_1\theta(k) + \frac{K_T T}{J}m(k), \\ \hat{x}_2(k+1) &= \frac{T}{2}(1 - K_2)\hat{\omega}(k) + (1 - 2K_2)\hat{x}_2(k) + K_2\theta(k). \end{aligned} \tag{13}$$

Since dynamics of the feedback control system and observer in Fig. 3. are decoupled, the speed of estimation of $\omega(k)$ may be adjusted by placing roots of the observer characteristic equation

$$z^2 + (K_1\frac{T}{2} + 2K_2 - 2)z + K_1\frac{T}{2} - 2K_2 + 1 = 0. \tag{14}$$

For example, gains K_1 and K_2 of the "dead-beat observer" are obtained from (14) by solving equations

$$\begin{aligned} K_1\frac{T}{2} + 2K_2 - 2 = 0, \\ K_1\frac{T}{2} - 2K_2 + 1 = 0 \end{aligned} \tag{15}$$

for K_1 and K_2 to get $K_1 = 1/T$ and $K_2 = 3/4$. Due to a substantial sensitivity of the observer with dead-beat dynamic with respect to the measuring noise, such observer cannot be applied. As it has been suggested [5], the proper way for setting of observer gains consists in assuming the observer dynamic to be two to four times faster than, the dynamic of the adjoined closed-loop control system. Thus, since the bandwidth of the system in. Fig. 1. is $50Hz$, we assume the bandwidth of observer to be $f_c = 100Hz$. Consequently, the observer characteristic equation becomes

$$(z - \sigma_z)^2 = 0 \tag{16}$$

with $\sigma_z = \exp(-2\pi f_c T) = 0.8282$. By equating identically corresponding coefficients of equations (14) and (16), we arrive at

$$\begin{aligned} K_1 &= \frac{1}{T}(\sigma_z^2 - 2\sigma_z + 1), \\ K_2 &= -\frac{1}{4}\sigma_z^2 - \frac{1}{2}\sigma_z + \frac{3}{4}, \end{aligned} \tag{17}$$

or $K_1 = 98.3793$ and $K_2 = 0.1644$, for $\sigma_z = 0.8282$. The system with designed identity observer is shown in Fig. 5.

Recall, for the estimation of shaft speed, the least complicated algorithm is based on the same form as the differential calculus limit definition of the derivative

$$\hat{\omega}(k) = \frac{\theta(k) - \theta(k+1)}{T} \tag{18}$$

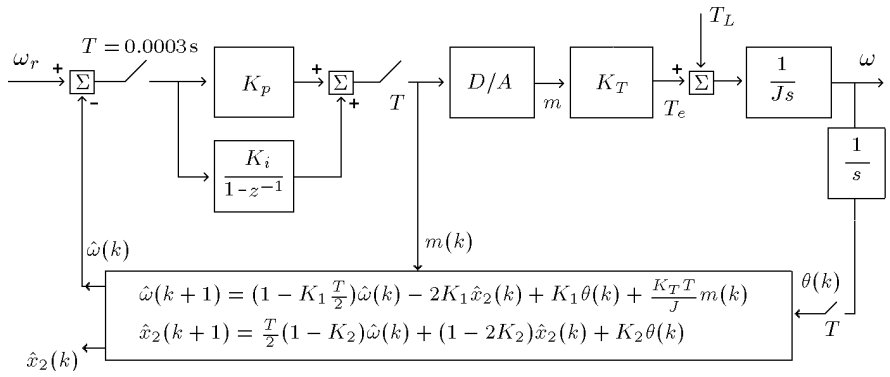

Fig. 5. Structure of speed-controlled electrical drive with ordinary identity observer

where $\theta(k)$ is the measured shaft angle position and T is the sampling period. The speed–controlled system with the feedback signal $\hat{\omega}(k)$ estimated by relation (18) was simulated first and results of the simulation run are shown in Fig. 6. Notice from Fig. 6., due to quantization effects, ripple changes appear in both the estimated shaft speed and torque command. These changes produce fluctuations in controlled variable (motor speed) and certain practical difficulties: the shaft speed and position are not smooth as necessary and motor losses increase due to the pulsation current. Then, the observer–based system in Fig. 5. with $(K_P, K_I) = (1.1453, 0.0539)$, $(K_1, K_2) = (98.3793, 0.1644)$, $K_T T/J = 0.15$, and $J = 0.002\ kg \cdot m^2$ was simulated taking into account the 12–bit resolution of the digital controller and resolver–to–digital converter within the position transducer. Results of simulation runs are shown in Figs. 7., 8. and 9. Figs. 7. and 8. demonstrate the ability of observer to remove ripples in the torque command. The efficiency of the shaft speed estimation is shown in Fig. 8. Notice from the step response in Fig. 7. and corresponding observed velocity in Fig. 9. that responses of the sistem and observer are in agreement with the requied speed of response, stability margin, and quality of estimation with respect to the accuracy, speed of estimation, and sensitivity to quantization noise.

As it is well known [4,5] the identity observer of such a kind is not able to estimate state variables in the presence of constant or slow varying load torque disturbances that may not be considered as initial values of state variables. This fact is visualized by Fig. 9., where the upper trace shows the estimated shaft speed for $T_L \equiv 0$; the lower trace, obtained for constant

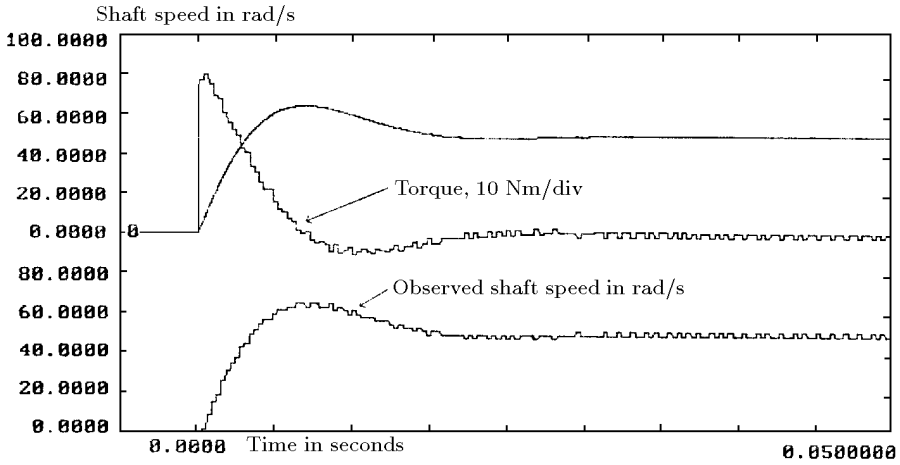

Fig. 6. Step response, electrical torque, and observed shaft speed of the system with least complicated velocity estimation

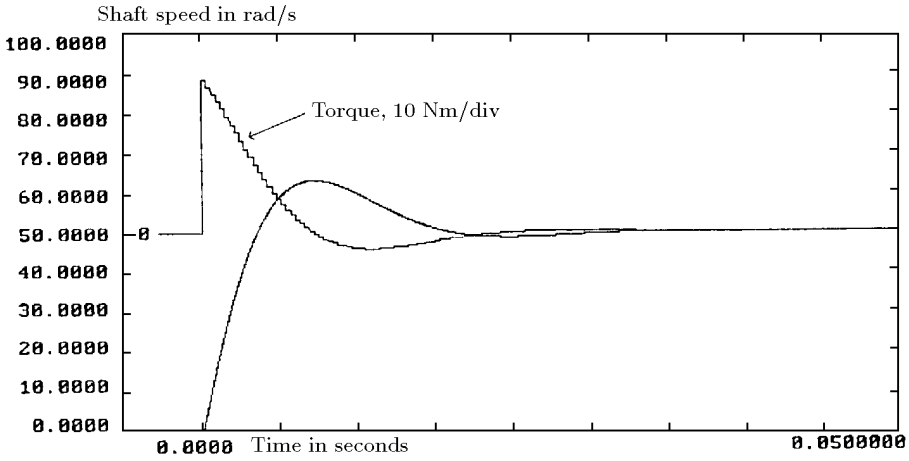

Fig. 7. Step response and electrical torque of the system with identity observer

load torque $T_L = 10Nm$, shows that the process of speed estimation brakes down in both the transient and steady–state conditions.

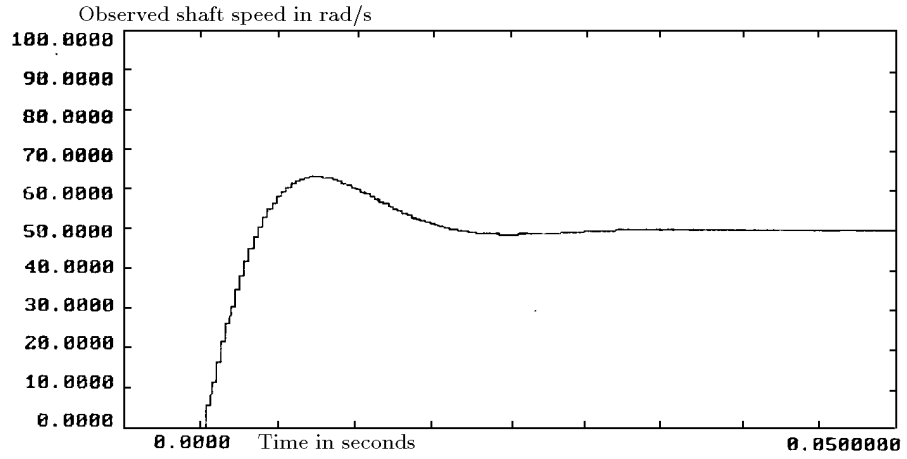

Fig. 8. Observed shaft speed in the system with identity observer

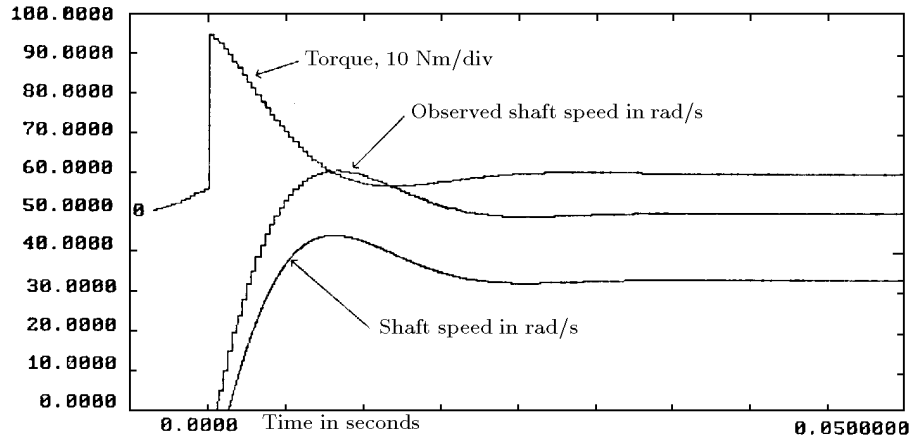

Fig. 9. Step response, electrical torque, and observed shaft speed of the system in the presence of a constant load torque disturbance

4. Design of Extended Observer

To enable the correct estimation in the presence of a constant or slow varying load torque disturbance, it is first necessary to transform observer

equations (13) by using relationships $x_2(k) = \frac{1}{2}\theta(k) - \frac{T}{4}\omega(k)$ and $\theta(k) = x_2(k+1) + x_2(k)$ [see Fig. 4.(b)] to obtain:

$$\begin{aligned} \hat{\omega}(k+1) &= \hat{\omega}(k) + K_1[\theta(k) - \hat{\theta}(k)] + \frac{K_T T}{J} m(k), \\ \hat{x}_2(k+1) &= \frac{T}{2}\hat{\omega}(k) + \hat{x}_2(k) + K_2[\theta(k) - \hat{\theta}(k)], \\ \hat{\theta}(k) &= \hat{x}_2(k+1) + \hat{x}_2(k). \end{aligned} \tag{19}$$

Notice that in Eqs. (19) the estimation error $\hat{e} = \theta(k) - \hat{\theta}(k)$ appears explicitly and that the observer may be employed for both the estimation of shaft speed $\omega(k)$ and filtering of measured shaft angle position $\theta(k)$.

After applying z-transform, Eqs. (19) can be rewritten, by simple rearrangements, into the matrix form

$$\begin{bmatrix} z-1 & 0 & K_1 \\ -\frac{T}{2} & z-1 & K_2 \\ 0 & z+1 & -1 \end{bmatrix} \begin{bmatrix} \hat{\Omega}(z) \\ \hat{X}_2(z) \\ \hat{\Theta}(z) \end{bmatrix} = \begin{bmatrix} K_1\Theta(z) + \frac{K_T T}{J} M(z) \\ K_2\Theta(z) \\ 0 \end{bmatrix}. \tag{20}$$

In virtue of (20), the observer characteristic equation can be calculated from

$$\Delta_c(z) = \begin{vmatrix} z-1 & 0 & K_1 \\ -\frac{T}{2} & z-1 & K_2 \\ 0 & z+1 & -1 \end{vmatrix} = 0 \tag{21}$$

to obtain its polynomial form

$$(1+K_2)z^2 + (K_1\frac{T}{2} - 2)z + K_1\frac{T}{2} - K_2 + 1 = 0. \tag{22}$$

For adjustment of observer gains, the same procedure as in the case of observer (13) may be carried out. Hence, equating identically corresponding coefficients of Eqs. (16) and (22), one obtains

$$\frac{K_1\frac{T}{2} - 2}{1+K_2} = -2\sigma_z \text{ and } \frac{K_1\frac{T}{2} - K_2 + 1}{1+K_2} = \sigma_z^2 \tag{23}$$

with $\sigma_z = \exp(-2\pi f_c T)$, where f_c is the desired bandwidth of observer. Solving Eqs. (23) for K_1 and K_2, we get

$$K_1 = \frac{4}{T\Delta}(\sigma_z^2 - 2\sigma_z + 1), \quad K_2 = -\frac{1}{\Delta}(\sigma_z^2 + 2\sigma_z - 3) \tag{24}$$

with $\Delta = (\sigma_z + 1)^2$. For example, if $f_c = 100Hz$, Eqs. (24) yield $K_1 = 117.7437$ and $K_2 = 0.1968$.

As well as the ordinary identity observer designed in the preceding section, the observer (19) cannot be used in the presence of load torque disturbances. To enable the estimation of $\omega(k)$ and filtering of $\theta(k)$; when constant or slow varying load torque disturbances exist, the observrer equations (19) are extended by adding the integration state variable, which eliminates the steady-state integration error due to a constant load torque. The idea of introducing of an, integral action within the structure of ordinary identity observer commonly used in controlled electrical drives has been primarily suggested in [4]. After introducing of the integration state $\hat{u}_i(k)$ into (19), the equations of extended observer become:

$$\begin{aligned}
\hat{\omega}(k+1) &= \hat{\omega}(k) + K_1[\theta(k) - \hat{\theta}(k)]\hat{u}_i(k) + \frac{K_T T}{J} m(k), \\
\hat{x}_2(k+1) &= \frac{T}{2}\hat{\omega}(k) + \hat{x}_2(k) + K_2[\theta(k) - \hat{\theta}(k)], \\
\hat{\theta}(k) &= \hat{x}_2(k+1) + \hat{x}_2(k), \\
\hat{u}_i(k) &= \hat{u}_i(k-1) + K_3[\theta(k) - \hat{\theta}(k)].
\end{aligned} \tag{25}$$

To evaluate the characteristic equation of extended observer, the same procedure, as in the case of basic observer equations (19), may be applied. Carrying out the procedure, we arrive to the following equation of extended observer, in the matrix form equivalent to (20),

$$\begin{bmatrix} z-1 & 0 & K_1 & -1 \\ -\frac{T}{2} & z-1 & K_2 & 0 \\ 0 & z+1 & -1 & 0 \\ 0 & 0 & K_3 & 1-z^{-1} \end{bmatrix} \begin{bmatrix} \hat{\Omega}(z) \\ \hat{X}_2(z) \\ \hat{\Theta}(z) \\ \hat{U}_i(z) \end{bmatrix} = \begin{bmatrix} K_1\Theta(z) + \frac{K_T T}{J} M(z) \\ K_2\Theta(z) \\ 0 \\ K_3\Theta(z) \end{bmatrix}. \tag{26}$$

Let us denote by $\Delta_c^*(z)$ the characteristic polynomial of extended observer. By comparing (20) and (26), one can easily conclude that $\Delta_c^*(z)$ is derived as

$$\Delta_c^*(z) = (1 - z^{-1})\Delta_c(z) + \frac{K_3 T}{2}(z+1). \tag{27}$$

After substitution $\Delta_c(z)$ from (21) into (27), the characteristic equation $\Delta_c^*(z) = 0$ can be reduced into the polynomial form

$$\begin{aligned}
(1+K_2)z^3 + (K_1\frac{T}{2} - K_2 + K_3\frac{T}{2} - 3)z^2 \\
+(-K_2 + K_3\frac{T}{2} + 3)z - K_1\frac{T}{2} + K_2 - 1 = 0.
\end{aligned} \tag{28}$$

The setting of gains (K_1, K_2, K_3) may be conveniently performed assuming all observer poles to be same and equal to $\sigma_z = \exp(-2\pi f_c T)$, where f_c denotes an assigned bandwith of the observer. Thus, equating coefficients of (28) and

$$(z - \sigma_z)^3 = 0, \tag{29}$$

we obtain:

$$\frac{K_1 \frac{T}{2} - K_2 + K_3 \frac{T}{2} - 3}{1 + K_2} = -3\sigma_z, \tag{30a}$$

$$\frac{-K_2 + K_3 \frac{T}{2} + 3}{1 + K_2} = 3\sigma_z^2, \tag{30b}$$

$$\frac{-K_1 \frac{T}{2} + K_2 - 1}{1 + K_2} = -\sigma_z^3. \tag{30c}$$

Solving Eqs. (30) for K_1, K_2 and K_3, we derive a suitable relation for caiculation of optimal observer gains,

$$\begin{bmatrix} K_1 \\ K_2 \\ K_3 \end{bmatrix} = \begin{bmatrix} \frac{T}{2} & -1 + 3\sigma_z & \frac{T}{2} \\ 0 & -1 - 3\sigma_z^2 & \frac{T}{2} \\ -\frac{T}{2} & 1 + \sigma_z^3 & 0 \end{bmatrix}^{-1} \begin{bmatrix} 3 - 3\sigma_z \\ -3 + 3\sigma_z^2 \\ 1 - \sigma_z^3 \end{bmatrix}. \tag{31}$$

Equation (31) was used to calculate numerical values of optimal observer gains for the desired observer bandwidth f_c. The calculated values are putted in Table 1.

Table 1. Optimal values of observer gains

Sampling period $T = 0.0003s$					
Opt. gains	$f_c = 100Hz$ $\sigma_z = 0.8282$	$f_c = 150Hz$ $\sigma_z = 0.7537$	$f_c = 200Hz$ $\sigma_z = 0.6859$	$f_c = 250Hz$ $\sigma_z = 0.6242$	Dead-beat $\sigma_z = 0$
K_1	353.2490	788.9010	1388.2000	2141.0000	40000.000
K_2	0.309	0.4830	0.6690	0.8670	7.000
K_3	22.127	73.8630	172.4100	330.2300	26666.667

Fig. 10. shows the speed-controlled servo system with extended observer. System was simulated with the constant load torque of $T_L = 10Nm$. In the simulation run, the values $(K_1, K_2, K_3) = (353.249, 0.309, 22.127)$ were used; values of controller and plant parameters stayed unchanged. Traces of Fig. 11. visualize the ability of extended observer to estimate correctly the shaft speed even in the case a constant load torque acts. Comparing Figs. 7., 8., and 11., one can conclude that a slight difference exists in the step responses and quality of estimation accomplished by the basic and extended observer.

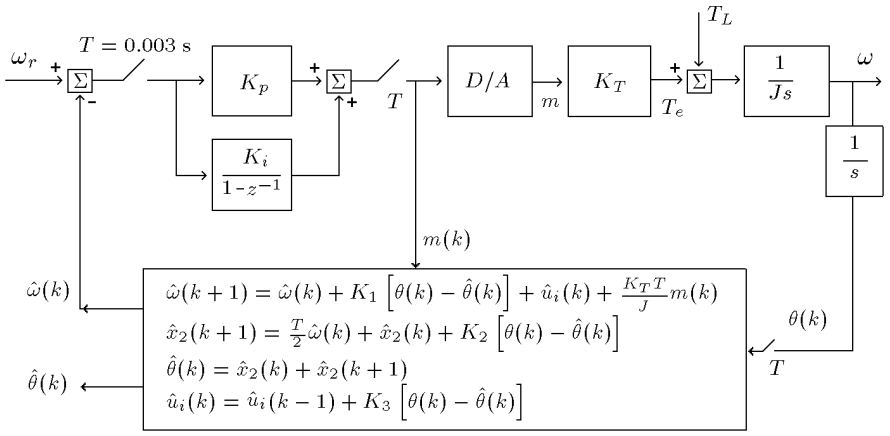

Fig. 10. Structure of speed-controlled electrical drive with the observer extended by the integration state

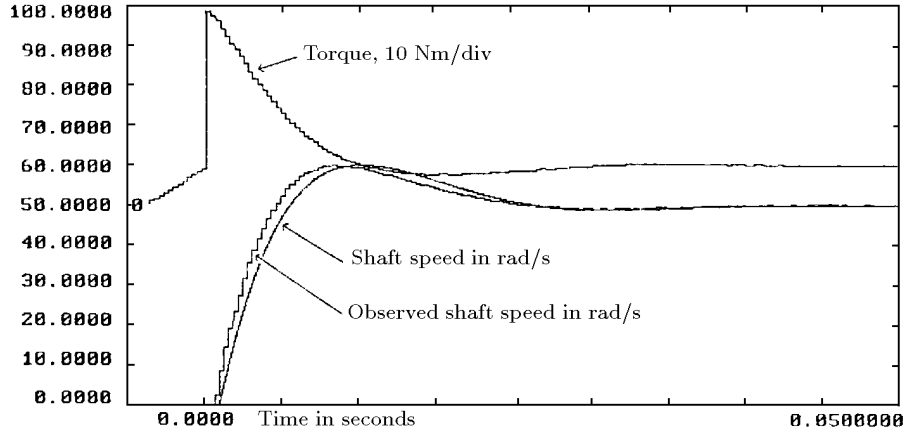

Fig. 11. Step response, electrical torque, and observed shaft speed of the system with extended observer and constant load torque disturbance

5. Conclusion

The structures of observer–based control systems and procedures of parameter setting, proposed in this paper, are verified by the computer sim-

ulation and checked by an experimental setup where the electromagnetic resolver was attached to the motor. The motor is rated$7Nm$, and the maximal speed is $3500rpm$. The R/D converter with resolution of 12-bit was used for deriving the shaft position from resolver signals. The proposed observer–based servo controllers were implemented on the microcontroller with the sampling time of $300\mu s$. Results of analytical design verified by simulation are in agreement with experimental investigations of the real system. Note that the suggested design procedure can be applied, with minor modifications, to controlled electrical drives with different kind of rotors.

REFERENCES

1. M. R. Stojić and S. N. Vukosavić: *Design of microprocessor-based system for positioning servomechanism with induction motor.* IEEE Transactions on Industrial Electronics, vol. 48, No. 5, October 1991, pp. 369–378.
2. S. N. Vukosavić and M. R. Stojić: *On–line Tuning of the rotor time constant for vector–controlled induction motor in position control applications.* IEEE Transactions on Industrial Electronics, vol. 40, No. 1, February 1993, pp. 130–138.
3. F. Blachke: *Das prinzip der feldorientirung die grundlage für die TRANSVEKTOR, regelung von drehfeld–maschinen.* Siemens Zeitschrift, vol. 45, No. 10, 1971, pp. 757–760.
4. R. D. Lorenz and K. Van Patten: *High resolution velocity estimation for all digital, AC servo drives.* in IEEE-IAS Conf. Rec. 1988, pp. 363–368.
5. M. R. Stojić: *Digital Control Systems.* Belgrade: Scientific Book, 1989 (in Serbian).
6. B. Friedland: *Control System Design.* McGraw–Hill, New York, 1986.
7. M. R. Stojić: *Design of microprocessor–based system for DC motor speed control.* IEEE Transactions on Industrial Electronics, vol. 31, No. 3, August 1984, pp. 243–249.